Bearing Capacity, Comparison of Results from FEM and DS/EN 1997-1 DK NA 2013

Bjørn Staghøj Knudsen
COWI A/S, Denmark, bskn@cowi.dk

Niels Mortensen
nmGeo, Denmark, n@nmgeo.dk

ABSTRACT
The bearing capacity of foundations in Denmark is typically analysed using the closed form equations from DS/EN 1997-1 DK NA:2013, and the present paper compares selected examples with similar results from the finite element method (FEM). The paper includes a discussion of the bearing capacity factors, the shape factors, plane strain considerations, axi-symmetry and three-dimensional analyses.

Keywords: Bearing capacity, Shape factors, DS/EN 1997-1 DK NA:2013, FEM, PLAXIS

1 INTRODUCTION

The present paper compares the bearing capacity estimated using DS/EN 1997-1 DK NA:2013 (EC7-DK NA) with results obtained using the finite element method (FEM). The overall scope is to investigate whether the two approaches will lead to similar bearing capacities. The paper summarises the main aspects covered in the report Banedanmark (2014).

1.1 Main assumptions

The main assumptions used in the investigations are: The base of the footing is placed on a horizontal soil surface comprising either a drained (sand) or undrained (clay) soil; The soil is isotropic and homogeneous; The Mohr-Coulomb failure criterion is applied using associated and non-associated flow; The foundation is loaded vertically with centrically and eccentrically loading included.

2 BEARING CAPACITY FORMULA

The drained bearing capacity formula contains three independent contributions that are calculated separately and added following equation (1). These three contributions are represented through the effective unit weight, γ', the effective surcharge q' and the effective cohesion, c'.
In this study the contributions are first investigated separately to examine the ability to recreate each of these using FEM, after which the combined effect is investigated.

2.1 Drained capacity

The overall drained bearing capacity formula from EC7-DK NA is given in equation (1).

$$\frac{Q_f}{A'} = \frac{1}{2} \cdot \gamma' \cdot B' \cdot N_\gamma \cdot s_\gamma + q' \cdot N_q \cdot s_q \qquad (1)$$

Where Q_f/A' is the vertical bearing capacity, B' is the effective foundation width, N_γ is the bearing capacity factor for the γ'-case with s_γ being the corresponding shape factor, N_q is the bearing capacity factor for the q'-case with and s_q being the corresponding shape factor. The c'-case is a mathematical reflection of the q'-case and is thus left out from this study and of equation (1).
The basis for equation (1) is the two-dimensional case with N_γ from Lundgren & Mortensen (1953), N_q from Prandtl (1920) and with $s_\gamma = s_q = 1.00$. When investigating three-dimensional cases, the empirical factors s_γ and s_q differs from unity. Therefore, the Danish approach with equation (1) is to use the plane strain friction angle, φ'_{pl} for sand in all the analyses; also for a square footing.

Following EC7-DK NA, the plane strain friction angle (secant value) for sand is defined by $\varphi'_{pl} = \varphi'_{tr} \cdot (1.00+0.10 \cdot I_D)$, where I_D is the density index. With $I_D = 1.00$: $\varphi'_{pl} = 1.10 \cdot \varphi'_{tr}$. The effective foundation width *B'* was suggested by Brinch Hansen (1970) to be estimated as B' = B – 2·e, where B is the width of the foundation and e is the eccentricity of the vertical load relative to the vertical centre line. This approach is used and investigated in the study.

2.2 Undrained capacity

In the undrained case, the bearing capacity is calculated as:

$$\frac{Q_f}{A'} = c_u \cdot N_c^0 \cdot s_c^0 + q \qquad (2)$$

Where c_u is the undrained shear strength, N_c^0 is the undrained bearing capacity factor, s_c^0 is the shape factor and *q* represents the total surcharge.

3 METHOD OF INVESTIGATION

Four different aspects are investigated for each of the γ'-case, the q'-case and the undrained case:

- Can 2D FEM be used to validate the bearing capacity factors from EC7-DK NA?
- Can 2D FEM be used to validate the approach with effective foundation width?
- Can axi-symmetrical FEM models be used to validate the shape factor for a square footing from EC7-DK NA?
- Can 3D FEM models be used to validate the shape factor for rectangular footings?

After investigation of each separate case the drained combined capacity is investigated with a case study using EC7-DK NA, plane strain and 3D models.

4 UNDRAINED CASES

The undrained analyses are based on a constant c_u = 10 kPa with Young's modulus, E = 20 MPa. The foundation is assumed weightless with E = 20 GPa. The interface between the soil and the foundation is modelled perfectly rough (10 kPa) or smooth (0.1 kPa).

4.1 Plane strain

A completely rough foundation was loaded vertically by a line load [kN/m] and the effect of different eccentricities was investigated. The load was increased until failure was observed and the bearing capacity factor was then back-calculated from equation (2): $N_c^{BC} = Q_f / (B' \cdot c_u)$. Table 1 summarizes the results from the FEM analyses. The analytical well-determined value of $N_c^0 = \pi + 2 \approx 5.14$.

Table 1: Plane strain Plaxis results for undrained clay. The value of "Acc." represents $N_c^{BC} / (\pi +2)$.

e [m]	B' [m]	e/B [-]	Q_f [kN/m]	N_c^{BC} [-]	Acc.
0.00	4.00	0.000	206.09	5.15	1.002
0.30	3.40	0.075	179.72	5.29	1.028
0.60	2.80	0.150	148.08	5.29	1.029
0.90	2.20	0.225	116.88	5.31	1.033
1.20	1.60	0.300	85.70	5.36	1.042
1.50	1.00	0.375	54.38	5.44	1.058

Table 1 shows that the bearing capacity factor can be accurately calculated using plane strain FEM, and that the effective foundation width concept is accurate within 5 % accuracy if e/B ≤ 0.30. Shear strain contour plots of selected failure mechanism from Table 1 are seen in *Figure 1*.

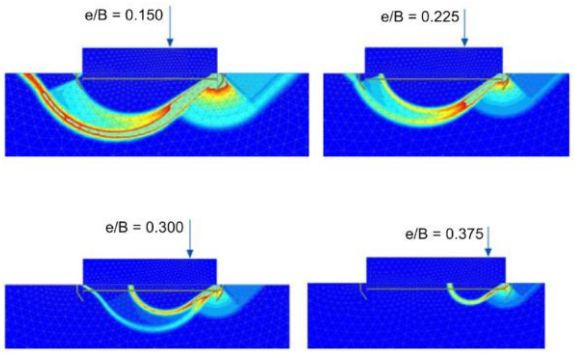

Figure 1 Shear strain contour plots for selected failure mechanisms in Table 1.

The interface strength did not influence the back-calculated bearing capacity factor.

4.2 Axi-symmetry

The axi-symmetric model was initially applied to investigate whether the interface strength would influence the estimated capacity. The back-calculated Plaxis result showed

N_c^{BC} = 6.06 where the theoretical solution implies 6.05, cf. Hansen (1982) and Martin (2004). For the smooth case, the Plaxis model gave 5.71 whereas the theoretical solution implied 5.67. The difference is likely due to the fact that "smooth" in the Plaxis-model was represented through an undrained shear strength of 0.1 kPa. The shear strain contour plots of the failure mechanisms are seen in Figure 2.

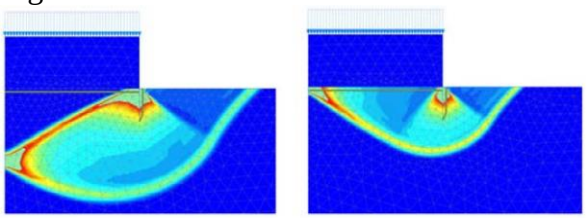

Figure 2: Shear strain contour plots for axi-symmetric failure mechanisms. Left: Completely rough and right: Smooth (0.1 kPa strength).

If the bearing capacity of a square footing equals the capacity of circular footing with the same area, the shape factor is thus s_s^0 = 6.06 / 5.14 = 1.18 for a perfectly rough foundation and 1.10 for a smooth foundation. EC7-DK NA uses s_c^0 = 1.0+0.2·B/L or corresponding to 1.20 for a square footing.

4.3 3D Models

The dependency between s_c^0 and the ratio B/L, where L is the foundation length, is investigated using Plaxis 3D models with a completely rough interface. The mesh of the 3D models include a quarter of the foundation (double symmetry). A vertical load is applied to the foundation, and failure is introduced through φ'-c-reduction. The following analyses are performed:

- A circular foundation in 3D Plaxis representing the axi-symmetrical case available in 2D Plaxis.
- A square footing (B = L).
- Five rectangular foundations (L > B) to investigate s_c^0.

The circular and square footings are compared to the results of the axi-symmetric results in Table 2.
From the results in Table 2 it can be concluded that estimating the bearing capacity of a circular foundation using either axi-symmetry or a 3D analyses leads to very similar results (deviation less than 3%). Furthermore, estimating the capacity of a square or circular footing with equal areas leads to almost identical results.

Table 2: Back-calculated results from Plaxis for circular and square foundations on undrained clay.

Plaxis model	N_c^{BC} [-]
Axi-symmetric (2D Plaxis)	6.06
Circular foundation (3D Plaxis)	6.22
Square foundation (3D Plaxis)	6.16

The results from the five rectangular footings are seen in Figure 3, in which the s_c^0-factor is back-calculated using $s_c^0 = Q_f / (A \cdot c_u \cdot (\pi+2))$.

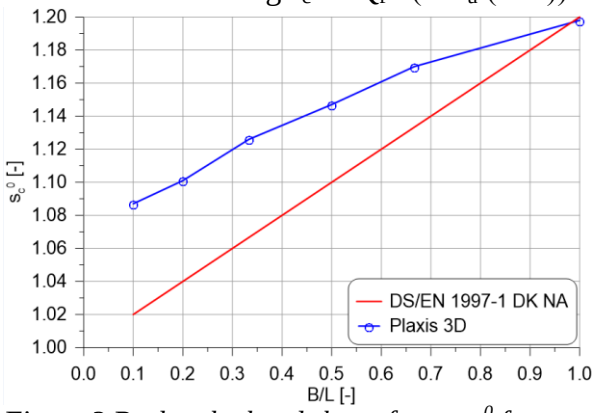

Figure 3 Back-calculated shape factor s_c^0 for undrained clay against the B/L-ratio based on Plaxis 3D results and EC7-DK NA.

Figure 3 shows that as the B/L-ratio decreases the results deviate more and more from EC7-DK NA. However even for B/L = 0.10 the difference is only 6.6 % with EC7-DK-NA being on the safe side, and the results from the two methods may thus be considered almost identical.

4.4 Conclusions

The main conclusions from the undrained analyses are as follows: The N_c^0 value can be estimated correctly using Plaxis 2D and the interface shear strength will not influence the bearing capacity. The adopted principle about the effective foundation width is confirmed up to e/B ≤ 0.30. The theoretical N_c^0 factor for axi-symmetry varies between 5.67 and 6.05 for a smooth and a completely rough interface, respectively. Almost similar results are found using Plaxis 2D models. Compar-

ing plane strain and axi-symmetry reveals a shape factor s_c^0 of 1.10 and 1.18 for smooth and completely rough interface, respectively. EC7-DK NA prescribes 1.20.
Plaxis 3D results indicate that the shape factor s_c^0 from EC7-DK NA is on the safe side.

5 DRAINED ANALYSES q'-CASE

Following equation (1), the drained capacity of a foundation placed on a soil with $\varphi' > 0$, $c' = 0$, $\gamma' = 0$ and a surcharge $q' > 0$ shall be estimated from $Q_f / A' = q' \cdot N_q \cdot s_q$ where the statically admissible solution of N_q is defined by $\tan^2(45°+\varphi'/2) \cdot e^{\tan\varphi'}$ and $s_q = 1.0+0.2 \cdot B/L$ following EC7-DK NA. The formula for N_q is only kinematically admissible for associated flow, i.e. $\varphi = \psi$.

5.1 Plane strain

The plane strain models were based on similar assumptions as for the undrained models except that the undrained shear strength was replaced by φ' and $c' = 0$.
For a vertical and centrally acting foundation load, the 2D Plaxis results were within a 0.5 % accuracy compared to the formula for N_q using φ' in the range of 15° to 45° with associated flow.
The interface shear strength did not influence the 2D Plaxis results.
For $\psi = \varphi' = 30°$, 2D Plaxis revealed $N_q^{BC} = 18.48$ to be compared with $N_q = 18.40$.
Setting $\varphi' = 30°$ and $\psi = 0°$, 2D Plaxis gave $N_q^{BC} = 14.50$ or 22 % reduction compared to associated flow.
Using a partial factor of $\gamma_{\tan\varphi'} = 1.20$ would give a reduction of 38 % for $\varphi' = 30°$. The difference between associated and non-associated flow is thus significant, albeit less significant than the effect of a partial factor of safety.
The influence of the eccentricity of the load was investigated similar to the undrained case, and the result can be seen in Table 3 for associated flow and $\varphi' = 30°$. The load was increased in the calculation until a fully developed failure mechanism occurred.
Table 3 shows that for $e/B < 0.25$ the bearing capacity estimated by Plaxis is up to 8 % higher, while the calculation with $e/B = 0.30$ shows a capacity that is lower than estimated using EC7-DK NA. It was not possible to obtain a failure for $e/B > 0.30$, as this lead to numerical problems.

Table 3: Plane strain Plaxis results for sand. Acc. is calculated as N_q^{BC} / N_q.

e [m]	B' [m]	e/B [-]	Q_f [kN/m]	N_q^{BC} [-]	Acc.
0.30	3.40	0.075	67.45	19.84	1.078
0.60	2.80	0.150	55.41	19.79	1.076
0.90	2.20	0.225	42.37	19.26	1.047
1.20	1.60	0.300	26.81	16.76	0.911

The principle of effective width represents an approximate approach for a drained material, and the accuracy is expected to increase for decreasing friction angles.
Shear strain contour plots of the failure mechanisms from Table 3 are seen in Figure 4.

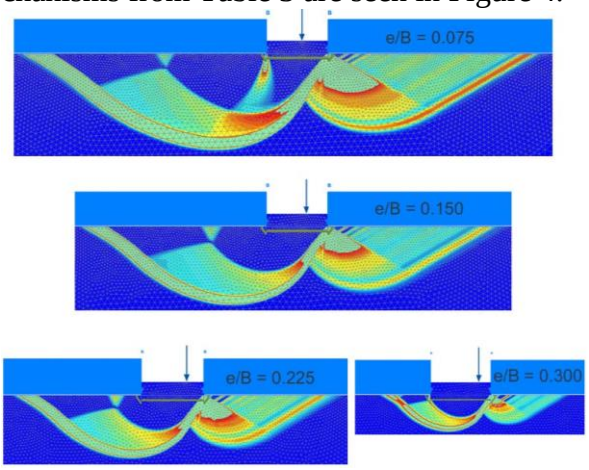

Figure 4 Shear strain contour plots of the failure mechanism investigated in Table 3. The plots are drawn to scale.

5.2 Axi-symmetry

For plane strain the N_q value is unambiguously defined and agreed upon in the literature. This is not the case with the axi-symmetric value of N_q. Albeit not representing a full literature study, some main points are summarized here.
The method of characteristics has been applied by Kumar & Ghosh (2005), Bolton & Lau (1993), Martin (2004) and Hansen (1979). The hoop stress in the model is assumed to be equal to the minor principal effective stress, σ'_3. $N_q = 29.5$ is obtained by Kumar & Ghosh (2005) and by Bolton & Lau (1993) using $\varphi' = \psi = 30°$. Martin (2004) arrives at $N_q = 37.2$ for the same assump-

tions, but he and Hansen (1979) states that the stress characteristics in the Rankine zone (see Figure 5) may cross each other, and the model applied can thus not represent a statically admissible solution.

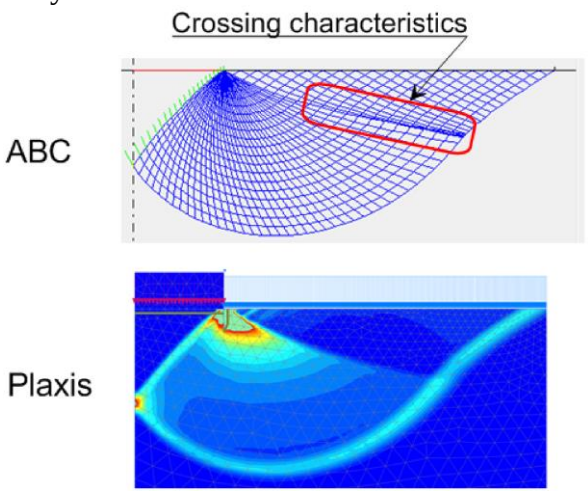

Figure 5 Upper part: Stress characteristics from Martin (2004) using a completely rough foundation base in an axi-symmetric analysis with φ' = ψ = 30°. Lower part: Shear strain contour plot from a similar Plaxis analysis. The plots are drawn to scale.

The observation from Martin (2004) with crossing stress characteristics is not mentioned by Kumar & Ghosh (2005) or by Bolton & Lau (1993), and Martin (2004) writes *"Certainly it appears that many previous researchers, including Cox et al. (1961), Cox (1962), Salençon & Matar (1982a) and Bolton & Lau (1993), have turned a blind eye to the occurrence of crossing characteristics in their meshes, if indeed they were aware of it at all"*.

The results from Martin (2004) do not deviate more than 2 % from similar results using Plaxis for friction angles between 15° and 45°. The approach from Martin (2004) yields almost identical results to those of Lundgren & Mortensen (1953) when calculating drained plane strain problems. In this paper it is therefore assumed that the approach applied by Martin (2004) leads to the "most realistic results".

The approach by Martin (2004) is established as a software code called ABC, which is available online with a documentation manual, enabling the user to calculate failure mechanisms for a wide range of input parameters.

For the q'-case, the shape factor s_q is investigated by the following approach:

- φ'_{tr} is varied from 10° to 45° and φ'_{pl} is estimated from $\varphi'_{pl} = 1.10 \cdot \varphi'_{tr}$.
- ABC is used to estimate the plane strain N_q^{pl} from φ'_{pl}, while N_q^{tr} is estimated from ABC and φ'_{tr}.
- The plane strain and axi-symmetric values are related with: $s_q \cdot N_q^{pl} = N_q^{tr}$.
- N_q^{tr} is estimated using Plaxis to compare.

The results of the investigation are seen in Table 4. N_q^{pl} is derived using φ'_{pl} as the rupture figure for N_q is a plain strain mechanism. A different approach will lead to different values of s_q.

Table 4: Estimated values of N_q using both plane and triaxial friction angles. Comparative axi-symmetrical Plaxis analyses are shown, using φ'_{tr} and associated flow.

φ'_{tr} [°]	φ'_{pl} [°]	N_q^{pl} [-]	N_q^{tr} [-]	N_q^{Plaxis} [-]
10.0	11.0	2.71	2.96	-
15.0	16.5	4.55	5.25	5.28
20.0	22.0	7.82	9.62	-
25.0	27.5	13.94	18.40	-
30.0	33.0	26.09	37.20	37.91
35.0	38.5	52.31	80.81	-
40.0	44.0	115.31	192.73	-
45.0	49.5	290.81	520.62	526.14

Table 4 shows that the values obtained from Plaxis using associated flow resembles those obtained from ABC using the method of stress characteristics. The formula below represents an approximation of the axi-symmetric N_q for a completely rough foundation. The regression coefficient is 0.99:

$$\log_{10}(N_q) = 5.035 \cdot 10^{-4} \cdot \varphi^2 + 3.487 \cdot 10^{-2} \cdot \varphi - 7.776 \cdot 10^{-2} \; [10° \leq \varphi \leq 45°]$$

EC7-DK NA dictates $s_q = 1.20$ for a square footing, independent of φ'. Figure 6 depicts the estimated relationship between s_q and φ' using data from Table 4, Brinch Hansen (1970) and data laboratory tests by de Beer (1970) where $s_q = 1.00 + B \cdot \tan(\varphi')/L$.

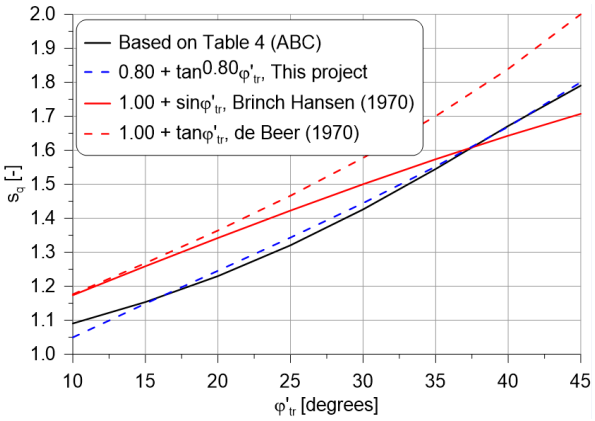

Figure 6: Estimated values of s_q from different approaches.

Using the approach from EC7-DK NA seems to be on the safe side as φ' ≥ ~17°. EC7-DK NA identifies $s_q = s_c$. However, s_c appears to be 10 to 20 % higher than s_q when s_c is evaluated using the procedures applied to estimate s_q.

5.3 3D Models

Modelling in Plaxis 3D were performed to validate the axi-symmetric results and to investigate the s_q factor as the ratio B/L is changed. The investigations were based on completely rough foundations, associated flow with φ' = ψ = 30° and c' = 0.
Failure in the models were found by displacement control. A circular, a square and three rectangular (B < L) foundations were investigated.
Results from the axi-symmetric, circular and square models are shown in Table 5.

Table 5: Back-calculated N_q values from Plaxis models. Martin (2004) estimates N_q = 37.20 for the same case.

Plaxis model	N_q^{BC} [-]
Axi-symmetric, Plaxis 2D	37.91
Circular footing, Plaxis 3D	39.55
Square footing, Plaxis 3D	38.86

Table 5 shows that the results of the axi-symmetric model and the circular foundation in Plaxis 3D leads to very similar values as the difference is less than 4 %. The value of the square footing is almost identical to the circular footing.
Back-calculating results of the Plaxis 3D models leads to an estimate of the s_q factor as seen in Figure 7. The expression from EC7-DK NA and results from de Beer (1970) is shown as well.

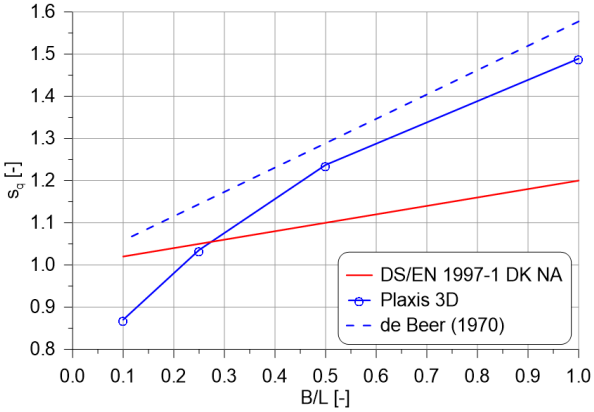

Figure 7: Back-calculated values of s_q for φ = 30° and associated flow.

Figure 7 indicates that the value of s_q from EC7-DK NA is on the safe side for φ' = 30° as the foundation length is below 3-4 times the width. When the length of the foundation exceeds 3-4 times the width the recommendation in EC7-DK NA may be on unsafe side. Results from de Beer (1970) generally show larger values of s_q than the other methods.
The reason for Figure 8 showing $s_q < 1$ for Plaxis 3D results may be due to different failure mechanisms occurring along the foundation. Close to the middle of the foundation the failure will be similar to the plane strain case, while at the ends of the foundation a more complex 3D failure mechanism occurs. This may lead to Plaxis 3D not being able to fully develop failure along the full length of the foundation as the capacity per length of foundation is not equal along the foundation.

5.4 Conclusions

Plane strain analyses with Plaxis leads to similar results as found in Prandtl (1920).
When applying non-associated flow a reduction of the estimated N_q of approximately 20 % is found. For eccentric vertical loads the approach in EC7-DK NA appears on the safe side of e/B < 0.25, for larger values the approach may be unsafe. Comparing plane strain and axi-symmetric models, the s_q value from EC7-DK NA may be unsafe for φ' lower than approximately 20°.
The shape factor from EC7-DK NA for L > B may be on the unsafe side when the founda-

tion length exceeds the width by 3-4 times. However this conclusion might be influenced by numerical issues.
The overall conclusion is that for the drained q'-case results from EC7-DK NA and Plaxis will likely deviate, with Plaxis giving the largest capacities. The size of the overshoot will depend on how the aspects covered in this paper are combined.

6 DRAINED ANALYSES γ-CASE

Following equation (1), the drained capacity for the γ'-case can be estimated from $Q_f / A' = ½ \cdot \gamma' \cdot B' \cdot N_\gamma \cdot s_\gamma$, where B' is the width or diameter of the footing and s_γ is the shape factor, $s_\gamma = 1.0 – 0.4\ B'/L$.
The plane strain value of N_γ was estimated by Lundgren & Mortensen (1953) using a statically admissible solution based on stress characteristics for a Mohr-Coulomb material. Bønding (1970) showed that the solution is kinematically admissible for a wide range of dilation angles ψ. EC7-DK NA includes the following approximation: $N_\gamma = ¼ \cdot ([N_q-1] \cdot \cos \varphi')^{3/2}$, valid for a completely rough interface.
The approach and assumptions described in the q'-case has been reused for the γ'-case, however with the soil weight γ' = 10 kN/m³ and q' = 0 kPa.

6.1 Plane strain

Initially N_γ was investigated using plane strain models. Due to numerical issues a surcharge of q' = 0.1 kPa was added and failure in the model was obtained by either increasing the load (Load) or by adding a prescribed displacement (Disp.). The back-calculated value N_γ^{BC} is found from equation (1) and shown in Table 6. The effect from the surcharge is removed from the Plaxis results.
The results in Table 6 for φ' = ψ = 30° indicate that displacement control may lead to the most accurate results. When using ψ = 0°, the capacity reduces about 20 %, similar to what was found in the q'-case.
The bearing capacity formula is based on superposition of each contribution, and if all the effects from γ', q' and c' are included in one and the same analysis, Lundgren & Mortensen (1953) showed that the estimated bearing capacity would increase by a factor μ being dependent on the ratio $\gamma' \cdot B/(q' + \gamma' \cdot B)$. This effect is not included in the present paper, but the effect can be observed in the results from 2D Plaxis too.

Table 6: Back-calculated plane strain results for sand for a completely rough foundation.

φ' [°]	ψ' [°]	Load-ing	N_γ^{BC} [-]	N_γ [-]	Acc. [-]
15	15	Disp.	1.26	1.18	1.070
30	30	Load	15.96	14.75	1.082
		Disp.	15.49		1.050
35	35	Disp.	36.86	34.48	1.069
30	0	Disp.	12.03	-	-

Table 6 includes analyses covering φ' up to 35° and numerical problems were encountered for higher values of φ'. With φ' = 40° and γ' = 10 kN/m³ the average pressure below a 4 m wide foundation is 1700 kPa, whereas the vertical effective stress on the soil surface next to the footing is 0 kPa. The stress singularity at the edge of the foundation is apparently too strong to allow for a numerical solution with the finite element method.
The effect of eccentric loading was investigated similar to the previous cases and the 2D Plaxis results revealed an overshoot of approximately 5 % for e/B < 0.25. For e/B > 0.25 numerical problems were encountered.

6.2 Axi-symmetry

When the literature is surveyed, the value of the axi-symmetric N_γ–value reveals a significant scatter. Results from Kumar & Ghosh (2005) and from Bolton & Lau (1993) are consistently higher than those values derived from Plaxis and ABC. Bolton & Lau (1993) and Kumar & Ghosh (2005) may not have assumed the critical shape of the failure mechanism.
The Plaxis results from Table 7 are approximately 7 % higher than those obtained from ABC. The lowest row in Table 7 represents a calculation using φ = 30° and ψ = 0°. The estimated capacity is approximately 25 % lower than for associated flow.

*Table 7: Results from ABC and Plaxis used to estimate the axi-symmetric value of Nγ for a completely rough foundation. * ψ = 0°.*

φ' [°]	ABC		Plaxis		Acc. [-]
	Q_f/A [kPa[	N_γ^{BC} [-]	Q_f/A [kPa]	N_γ [-]	
10	6.46	0.32	-	-	-
15	18.7	0.93	20.73	1.01	1.08
20	48.4	2.42	-	-	-
25	121.6	6.08	-	-	-
30	310.8	15.5	335.9	16.61	1.07
35	838.5	41.9	907.0	44.95	1.07
40	2474.5	123.7	-	-	-
45	8356.3	417.8	-	-	-
30*	-	-	249.5	12.29	

Figure 9 shows the shear strain contour plot from Plaxis using φ' = ψ = 35°. Using larger friction angles implied numerical problems.

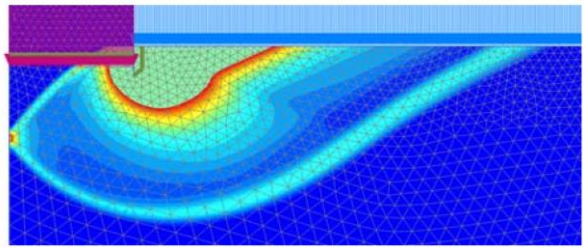

Figure 9: Shear strain contour plot of the axi-symmetric failure mechanism for associated flow, φ' = 30° and a completely rough foundation.

The results from ABC in Table 7 leads to the following approximation of N_γ for a completely rough foundation [10° ≤ φ' ≤ 45°]:

$$\log_{10}(N_\gamma) = 2.576 \cdot 10^{-5} \cdot \varphi^3 - 1.868 \cdot 10^{-3} \cdot \varphi^2 + 1.253 \cdot 10^{-1} \cdot \varphi - 1.581$$

The coefficient of regression is 0.9983.
The shape factor $s_\gamma^{L=B}$ was estimated using the same approach suggested for the q'-case: $s_\gamma^{L=B} = 2N_\gamma^{tr} / (N_\gamma^{pl} \cdot \sqrt{\pi})$, where $D/B = 2 \cdot \sqrt{\pi}$, N_γ^{tr} follows Table 7 and N_γ^{pl} is calculated from Lundgren & Mortensen (1953) with $\varphi'_{pl} = 1.10 \cdot \varphi'_{tr}$. These values are shown together in Figure 10.
In EC7-DK NA $s_\gamma^{L=B}$ is dictated as equal to 0.60 with no dependency on φ', this appears to be on the safe side.

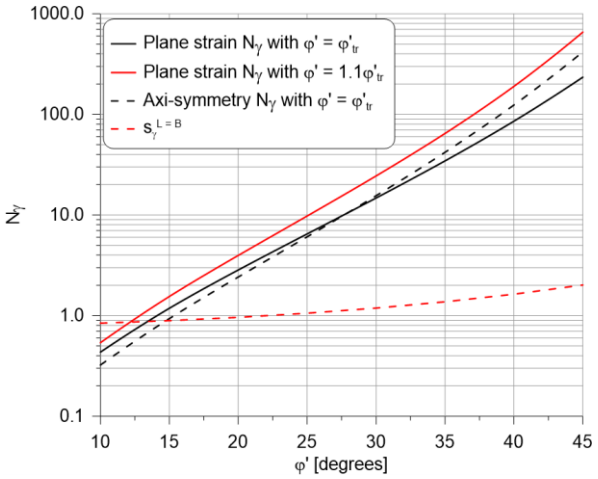

Figure 10: Estimated values of N_γ against the triaxial friction angle. Note that the dashed red curve represents $s_\gamma^{L=B}$ and not N_γ .

6.3 3D Models

The calculations in Plaxis 3D for the pure γ'-case proved to be very challenging to execute to a satisfactory level. As in the Plaxis 2D calculations, a small surcharge was applied to ensure non-zero effective stresses at the soil surface. This was however not enough to ensure stable and reliable calculation results. The results presented in this section are the product of a large number of iterations regarding modelling and numerical parameters, in the attempt to reproduce results similar to the axi-symmetric results and obtain reliable failure mechanism.
It seems that Plaxis 3D calculation for the pure γ'-case is not feasible, as this will lead to numerical issues and results that are not easily reproducible for varying numerical settings. The results of this section should thus be taken as a best estimate based on the work performed within the time frame of this project, and that further work is needed to fully understand the issues involved in executing reliable 3D FEM calculations for a pure γ'-case.
Using q' = 1.0 kPa, γ' = 10 kN/m³ and a diameter of D = 3.54 m, the results shown in Table 8 was obtained.
The failure load is divided by a combination factor μ = 1.18 for φ' = 15° and μ = 1.10 for φ = 30°, before N_γ is back-calculated. This combination factor accounts for the superposition effect of the γ' and q' contribution and is explained in Banedanmark (2014).

*Table 8: Back-calculated values of N_γ for a circular foundation with completely rough interface. * Result from Table 7.*

φ' [°]	Plaxis 3D		Plaxis 2D*	ABC
	Q_f/A [kPa]	N_γ [-]	N_γ [-]	N_γ [-]
15	29.62	1.12	1.01	0.93
30	532.74	25.26	16.61	15.54

Table 8 shows that the 3D models leads to comparable values for φ' = 15°, however for φ' = 30° the values differ by a factor 1.5.
Analyses for rectangular foundations (B<L) were undertaken, and the main results are seen in Table 9. The value of the combination factor μ is calculated based on Banedanmark (2014). The shape factor is calculated as: $s_\gamma = (Q_f/A/\mu - q' \cdot N_q) / (1/2 \cdot \gamma' \cdot B \cdot N_\gamma^{pl})$.
The results for L = B from Table 9 should be directly comparable to Figure 10 as the contribution from q' has been corrected for. For φ' = 15° the values are comparable, however for φ' = 30° they are not.

Table 9: Main results from Plaxis 3D analyses using rectangular foundations with B = 4 m and $\gamma' = 10$ kN/m³.

L [m]	q' [kPa]	φ' [°]	Q_f/A [kPa]	μ [-]	s_γ [-]
4	1.0	15	39.90	1.17	0.973
8	0.1		38.23	1.05	1.162
16			40.01		1.217
40			42.22		1.284
4	1.0	30	387.9	1.09	0.691
8			476.8		0.858
16			489.6		0.882

For the Plaxis 3D analysis with $\gamma' > 0$ and $q' \approx 0$ it has been difficult to identify a clear and consistent final state of failure. Increasing the value of q' will improve converge towards failure.
The singularity at the edge of the foundation is represented by a geometrical point being subjected to a significant foundation pressure at one side and to a stress state of virtually no pressure on the other side, which may cause numerical problems. These problems are present in the 2D and axi-symmetric models as well, however here they only represent a single point in the model, while in the 3D models the singularity is present around the whole circumference of the foundation. The investigation within the time frame available did not allow for a solution of this problem. It might be the case that more elements are needed or that a strength increase in the soil should be present at the points of singularity.

6.4 Conclusions

Plane strain analyses with Plaxis in the γ'-case leads to a bearing capacity factor resembling what can be found from Lundgren & Mortensen (1953) and from EC7-DK NA. The value of N_γ will change as the roughness of the interface is changed. Using non-associated flow will reduce the capacity found by approximately 20 % compared to associated flow for φ' = 30°. For eccentrically acting loads the estimated capacity from Plaxis 2D is approximately 5 % higher for $e/B < 0.25$ using the effective foundation area concept. For larger values of e/B the approach in EC7-DK NA may be unsafe. The theoretical bearing capacity factor N_γ for a circular foundation has been evaluated. It appears that the solution provided by Martin (2004) fits the results of Plaxis 2D. The shape factor s_γ for a square foundation has been found to be larger than given in EC7-DK NA, however the results cannot generally be verified by Plaxis 3D analyses. Plaxis 2D can be used to evaluate the pure γ'-case, however a value of $q' \approx 1.0$ kPa must be used to obtain reliable results. Using q' = 1.0 kPa in Plaxis 3D can be used to evaluate the tendency of s_γ, e.g. it increases with L/B. Back-calculating results from Plaxis 3D with q' = 1.0 kPa has however not turned out to lead to reliable and consistent results. The overall conclusion for the drained γ'-case investigated is that EC7-DK NA and Plaxis will deviate. Mechanisms for plane strain and circular foundations can be studied, but Plaxis 3D results for the pure γ'-case appears to represent a challenge and it is therefore not recommendable to apply Plaxis 3D for capacity calculations in a pure γ'-case. For practical applications however, a pure γ'-case is rarely encountered.

7 COMBINED DRAINED CAPACITY

The combined capacity of the q'- and γ'-case has been investigated in Banedanmark (2014).

The main conclusion are that the results from Plaxis calculations will include the combination factor μ, which is not a part of EC7-DK NA, and a larger capacity will thus be found from Plaxis analyses than using EC7-DK NA. The μ-factor is well-established for the plane strain case, and comparing results from EC7-DK NA and Plaxis 2D including the μ-factor leads to identical results.
The μ-factor is not established for the 3D case, so the influence is not easy to directly isolate. Furthermore the relation between φ'_{tr} and φ'_{pl} is not constant or well determined. Plaxis 3D results will yield a capacity between the values found from EC7-DK NA using respectively φ'_{pl} and φ'_{tr}.

8 CONCLUSIONS

When using Plaxis 2D plane strain to investigate the q'- and γ'-case independently, the bearing capacity factors fit well with EC7-DK NA for vertically acting central loads using associated flow. For eccentrically acting loads, the effective foundation concept is confirmed for a relative eccentricity of up to 0.2 to 0.3 depending on the actual case.
The shape factor s_q as defined in EC7-DK NA may be too high for $\varphi' < 20°$ and too low for $\varphi' > 20°$, using a square footing.
The shape factor s_γ defined in EC7-DK NA is lower than the value found by compared circular and square footings using Plaxis 2D and 3D, however small scale testing from de Beer (1970) supports the approach in EC7-DK NA. Bearing capacity factors for N_q and N_γ are established for circular foundations. Most authors agree in the value for N_q, but N_γ appears to be too high. The results from Martin (2004) fits well with those values established using Plaxis 2D. The results from Plaxis 3D show that the pure γ'-case cannot be analysed and a surcharge must be added. The plane strain effect with $\varphi'_{pl} > \varphi'_{tr}$ cannot be investigated in Plaxis 3D as the material models do not reflect this aspect, so φ'_{tr} must be used in Plaxis 3D. The bearing capacity estimated with φ'_{pl} and EC7-DK NA appears to be higher than found with Plaxis 3D and φ'_{tr}. Shape factors are empirical factors and deriving exact values by the finite element method will be influenced by the choice between φ'_{pl} and φ'_{tr}, the μ-factor and the element net applied.

9 FURTHER WORK

The 3D FEM results reveal a challenge when estimating the capacity for the γ'-case. More work should be undertaken in order to better understand this issue. It might be the case that the mesh used in the calculations is simply not fine enough to reproduce correct results or that other measures should be undertaken in order to handle to singularities at the edge of the foundation.

10 ACKKNOWLEDGEMENTS

The authors are grateful for being allowed to publish the work by Banedanmark.

11 REFERENCES

Bolton, M.D. & C.K. Lau (1993). Vertical Bearing Capacity Factors for Circular and Strip Footings on Mohr-Coulomb Soil, Canadian Geotechnical Journal, Volume 30, pp. 1024-1033.

Hansen, Bent (1982). Geoteknik og Fundering III, 1982, Notat 24, Særlige problemer.

Brinch Hansen (1970). A Revised and Extended Formula for Bearing Capacity, Bulletin 28, The Danish Geotechnical Institute, Copenhagen 1970.

Bønding, N. (1977). Kinematically Admissibility of the Pure N_γ Rupture Figure, Proceedings of the Ninth International Conference on Soil Mechanics and Foundation Engineering, 1977, Tokyo.

de Beer, E.E. (1970), Experimental Determination of Shape Factors and the Bearing Capacity Factors of Sand, Geotechnique 20, Number 4, 387-411.

DS/EN 1997-1, Eurocode 7: Geotechnical Design– Part 1: General Rules, Danish National Annex 2013 included.

Kumar, J. & P. Ghosh (2005). Determination of N_γ for Rough Circular Footings Using the Method of Characteristics, Electronic Journal of Geotechnical Engineering, Paper 2005-0540

Lundgren, H. & K. Mortensen (1953). Determination by the theory of Plasticity of the bearing capacity of Continuous Footings on Sand, Proc. 3rd Int. Conf. Soil Mech., Volume 1, p. 409, Zürich 1953.

Martin, C.M. (2004). User's Guide, ABC - Analysis of Bearing Capacity, Version 1.0, Department of Engineering Science, University of Oxford, OUEL Report No. 2261/03.

Prandtl, L. (1920). Über die Härte plastischer Körper, Nachr. D. Ges. D. Wiss., math-phys. Kl. Göttingen 1920.